

New Higgs interactions and recent data from the LHC and the Tevatron

Shankha Banerjee¹, Satyanarayan Mukhopadhyay² and Biswarup Mukhopadhyaya³
Regional Centre for Accelerator-based Particle Physics
Harish-Chandra Research Institute
Chhatnag Road, Jhusi, Allahabad - 211 019, India

Abstract

We perform a multi-parameter global analysis of all data available till date from the ATLAS, CMS and Tevatron experiments, on the signals of a Higgs boson, to investigate how much scope exists for departure from the standard model prediction. We adopt a very general and model-independent scenario, where separate deviations from standard model values are possible for couplings of the observed scalar with up-and down-type fermions, W-and Z-boson pairs, as well as gluon and photon pair effective interactions. An arbitrary phase in the coupling with the top-pair, and the provision for an invisible decay width for the scalar are also introduced. After performing a global fit with seven parameters, we find that their values at 95% confidence level can be considerably different from standard model expectations. Moreover, rather striking implications of the phase in top-quark coupling are noticed. We also note that the invisible branching ratio can be sizeable, especially when the couplings of the Higgs to W-and Z-pairs are allowed to be different.

¹E-mail: shankhaban@hri.res.in

²E-mail: satya@hri.res.in

³E-mail: biswarup@hri.res.in

1 Introduction

The recent announcements on Higgs boson search from the 2012 run of the Large Hadron Collider (LHC) [1, 2], in conjunction with earlier results, have brought a refreshing gale into the stultified arena of particle physics, starved of breakthrough for several decades. Physicists tend to concur that both the CMS and ATLAS collaborations have found a spin-zero bosonic resonance of mass 125 - 126 GeV. However, the issue of whether it is exactly the Higgs boson predicted by the standard electroweak model (SM) [3, 4] is still somewhat open. This question can be settled by the close examination of accumulating data over a longer period, thus revealing not only the complete picture of the electroweak symmetry breaking sector but also any secret message of new physics buried within the available results.

Any departure from SM predictions in the observed scalar is ultimately reflected in its interactions with pairs of fermions or weak gauge bosons, and also the loop-induced effective couplings to photon and gluon pairs. However, these interactions are rather intricately twined in the calculation of rates for various final states into which the Higgs can decay. The trace of non-standard physics there can be looked for in two ways— either in the context of specific theories where the different new couplings are all dictated by the model parameters, or in a phenomenological, model-independent analysis of as general a nature as possible. We attempt to add the present investigation in the second direction, to the already growing volume of extant studies in the light of the data piling up [5, 7, 8].

We start by assuming that the $SU(2)_L \times U(1)_Y$ gauge invariance holds at the energy scale under scrutiny. Under such circumstances, the aforementioned interactions of the Higgs boson can be different from the SM expectations due to (a) the observed scalar having admixtures with other states, or (b) the presence of additional, gauge invariant effective operators which contribute to the same couplings. In either case, a renormalisation of the SM couplings may take place, and interactions with new Lorentz structure may also appear. Only the former possibility is addressed in the present work.

The modification of the SM couplings of the Higgs is subject to various experimental constraints, the severest of them often coming from electroweak precision observables. Our purpose is to investigate, within such constraints, how much allowance for departure of various interaction strengths from the SM values can be made by the currently observed rates in different final states, as found from a global fit of these strengths based on chi-square minimisation. The available best fits for the rates in different channels, scaled by the corresponding SM expectations, are our inputs, and we use them to obtain the widest allowed ranges for various modified couplings as well as an invisible decay width, with the hope that this will guide us to the direction where new physics may lie.

We start by assuming that the Higgs (or, to be more precise, the observed boson, to which we refer here as the Higgs) can differ from the SM expectations in all respects— couplings with $T_3 = +1/2$ and $T_3 = -1/2$ fermions (the departures being different in the two cases), couplings with both W- and Z-boson pairs (again with potentially different deviations), and also the effective couplings to photon and gluon pairs, where additional effects over and above the modified fermion and boson couplings are included as possibilities. While the modifications mentioned above can be described in terms of a given framework (such as a chiral Lagrangian), we deliberately take them as completely free and independent parameters, to make our study free of any theoretical bias. Besides, it is also assumed at the

beginning that the Higgs can have a finite invisible decay width. We use the CMS as well as ATLAS results in various channels for both the 2011 (7 TeV) and 2012 (8 TeV) runs [9]. Results from the Tevatron, wherever available, are also used as data points in obtaining the least-square fits [10].

As has been already mentioned, a number of similar investigations have appeared in the literature [8]. Though they are all instructive, the present study may be of particular use in the following respects:

- We start by taking *all* of the couplings, tree-level as well as loop-induced, to be unrelated and free parameters. The couplings to up-and down-type quarks, as also those to W-and Z-pairs, are allowed to be different at the same time. Most earlier studies (except, for example, Refs. [5] and [6]) have not allowed uncorrelated variation of HWW and HZZ interactions, albeit in a gauge-invariant fashion; also, some of them set the interactions with up-and down-type quarks to identical value.
- We investigate the effect of an arbitrary phase in the fermion pair couplings, relative to the W-pair couplings, which is also varied as a free parameter in obtaining the global fits.
- We do not restrict ourselves by assuming the anomalous interactions to arise from some underlying scenario like a chiral Lagrangian, which implies concomitant variation of different couplings.
- We take into account the possibility that the effective Hgg and $H\gamma\gamma$ couplings are modified due to effects other than non-standard interactions of the Higgs with W-and fermion pairs. Furthermore, the possibility of loop-induced Higgs decays being modified differently due to both coloured and colourless fermions running in the loops is taken into consideration. We keep the modifications due to these two different effects separate and uncorrelated.
- An invisible decay width for the Higgs is allowed as a free parameter.
- We parametrize all new physics effects at the coupling level (excepting for the invisible width, where we take the width as a free parameter, for the sake of model-independence). This is in contrast to cases where branching ratios of the Higgs into some channels are taken as free parameters, which results in various new physics effects getting entangled, since branching ratios also involve the total decay width of the Higgs, where all (modified) interactions contribute.
- In obtaining the 2σ ranges of allowed values for various couplings, we have fixed the remaining parameters not at their SM values but at their global best fits corresponding to the minimum of the χ^2 function. This makes our analysis completely unbiased, from the angle of physics beyond the SM.
- Even in channels where the gluon fusion channel for Higgs production dominates, the vector boson fusion (VBF) and associated production channels contaminate the rates to varying degrees. Also, the VBF and associated channels have both HWW -and

HZZ -induced contributions. These warrant a careful treatment if one is allowing uncorrelated deviations from SM in the HWW and HZZ interactions. Difficulties on this front are compounded by different efficiency of cuts in different channels. Such issues have been taken into account in our analysis.

- In cases where only the 2011 data are used, where the best fit values for various rates come with asymmetric error-bars, the asymmetry is retained in the analysis that follows.

In section 2, we outline our parametrization of the various new physics effects mentioned above, and discuss the motivations of their origin. The details of input data sets from the LHC and the Tevatron used in our global numerical analysis, and the methodology adopted have been described in section 3. We discuss our results of the best-fit values obtained and the allowed confidence intervals for the various parameters in section 4. We summarise and conclude in section 5.

2 New physics effects: parametrization

In this section, we describe the parameters used to encapsulate any likely new physics effect hidden within the data on the Higgs. We also outline the motivations for choosing these parameters, and indicate the ranges over which we let them vary to obtain their favoured locations in the light of observations till date.

Fermion couplings

Classifying all $T_3 = +1/2$ fermions as u , and all $T_3 = -1/2$ fermions as d , we assume

$$\begin{aligned}\mathcal{L}_{H\bar{u}u}^{eff} &= e^{i\delta}\alpha_u\frac{m_u}{v}H\bar{u}u \\ \mathcal{L}_{H\bar{d}d}^{eff} &= \alpha_d\frac{m_d}{v}H\bar{d}d\end{aligned}\tag{1}$$

where H denotes the scalar with a Higgs-like appearance. This parametrization implicitly assumes the couplings of H to all fermions to be proportional to their masses. The assumed difference in interaction strengths to up-and down-type fermions include the possibility of H being part of a scenario containing more than one doublets, including the supersymmetric case. In general, a relative phase between the couplings is assumed¹. This phase allows various degrees of interference among fermion loops, and between the fermion and W-boson

¹A phase in the $Ht\bar{t}$ effective coupling can arise due to imaginary (absorptive) parts coming from loop diagrams for the transition where some of the intermediate SM states in the loop graphs, being lighter than the Higgs boson, can go on-shell. For example, a heavy W' like gauge boson having $W'tb$ type couplings can give rise to additional contributions to the $Ht\bar{t}$ effective coupling, via a triangle loop involving two b-quarks, where the b-quarks can go on-shell inside the loop. This would then give rise to an imaginary part in the effective interaction.

loops, for example, in the decay $H \rightarrow \gamma\gamma$. As will be seen in the next section, we perform a scan over the phase δ like we do over α_u and α_d . Even in cases where we neglect a non-trivial phase, we allow α_u and α_d to be both positive and negative, in order to account for constructive as well as destructive interferences. Moreover, the phase δ enters seriously into Higgs phenomenology only via the top quark couplings. Therefore, nothing is affected by dropping it for the first two families, in case it is subject to any constraints from flavour physics.

There are essentially no limits on $|\alpha_u|$ and $|\alpha_d|$ from earlier data, except those from perturbativity of the Yukawa couplings. Keeping this in mind, we take the maximum value of $|\alpha_u|$ to be 2 (keeping the top quark Yukawa coupling in mind), while $|\alpha_d|$ is *prima facie* allowed to lie all the way upto 40. However, even before the full analysis is done, we find that the rate for $H \rightarrow \gamma\gamma$ for large $|\alpha_d|$ gets suppressed well below limits admissible by current observations, as the $b\bar{b}$ mode then dominates overwhelmingly. With this in view, we also limit the maximum value of $|\alpha_d|$ to 2 in our final analysis. Since this renders the contribution of all $T_3 = -1/2$ SM fermions to $\Gamma(H \rightarrow \gamma\gamma)$ negligibly small, we also do not miss anything by dropping the phase in α_d . Note that the same consideration prevents us from taking seriously regions of the parameter space, where the b-quark loop contributes substantially to the gluon fusion channel of Higgs production. Thus we do not expect the phase in $Hb\bar{b}$ coupling, too, to affect Higgs production cross-sections.

Gauge boson pair couplings

We parametrize the interactions of the observed scalar to a pair of weak gauge bosons as

$$\begin{aligned}\mathcal{L}_{HWW}^{eff} &= \beta_W \frac{2m_W^2}{v} H W_\mu^+ W^{\mu-} \\ \mathcal{L}_{HZZ}^{eff} &= \beta_Z \frac{m_Z^2}{v} H Z_\mu Z^\mu\end{aligned}\tag{2}$$

where the Lorentz structure of the interaction has been tentatively taken to be the same as in the standard model. It should be emphasized that this parametrization, especially allowing $\beta_W \neq \beta_Z$, allows one to address the apparent suppression of the WW channel as opposed to the ZZ channel, as evinced in the 2011 data. Such anomalous interactions can arise if, again, the Higgs has admixtures of other doublets or scalars in some other representations of $SU(2)$, and also via loop effects in specific models.

Clearly, one faces precision electroweak constraints here, in particular, for $\beta_W \neq \beta_Z$, which entails a breakdown of custodial $SU(2)$, and is thus restricted by the T-parameter. Such anomalous couplings can arise, for example, from gauge invariant effective operators, an example being [11]

$$\mathcal{O}_\phi = \frac{f_\phi}{\Lambda^2} (D_\mu \Phi)^\dagger \Phi \Phi^\dagger (D_\mu \Phi)\tag{3}$$

where Φ is a set of $SU(2)$ doublet scalars, out of which H is the lightest mass eigenstate, and Λ is the scale below which the effective operator is defined. This operator in itself gives rise to unequal β_W and β_Z . However, taking this operator alone, precision constraints yield the limits [11, 12]

$$0.991 \lesssim \beta_W \lesssim 1.001 \quad (4)$$

$$0.997 \lesssim \beta_Z \lesssim 1.028 \quad (5)$$

It is hardly expected to see any appreciable effects of such variation on observable rates, and we do not include the bounds given by Eqns. 4, 5 in our global fits. However, one can have less constrained couplings if one includes other effective operators which, however, give rise to additional HWW and HZZ interactions involving derivatives. We do not rule out such possibilities, but neglect the effects of derivative couplings for the time being, and vary β_W and β_Z between 0 and 2, in a purely phenomenological way. An analysis including the derivative couplings will be presented in a subsequent study. We also consider the case where $\beta_W = \beta_Z \equiv \beta$, thereby restoring tree-level custodial invariance. In this case, for a Higgs mass of 125 GeV, electroweak precision constraints restrict β in the range [5]

$$0.84 \leq \beta^2 \leq 1.4 \quad (6)$$

Effective gluon-gluon and photon-photon couplings

The gluon fusion channel is the dominant production mode for a Higgs of mass around 125 GeV, and is overwhelmingly driven by the top quark loop. Therefore, a departure of α_u from unity will be reflected in the production cross-section (though the phase δ will be ineffectual). Similarly, the two-photon amplitude, which is responsible for perhaps the most discussed final state nowadays, has contributions from both fermion- and W -induced loops. Thus the parameter β_W also dictates the rate for the two-photon final state.

This is, however, not the entire story. Both of the aforementioned loop-induced processes can have modified contributions, beyond the coverage of the α - and β -parameters, if additional states contribute in the loops. The most obvious example is the contribution of Kaluza-Klein towers in theories with extra compact dimensions, where fermions and/or gauge bosons propagate in the bulk. Due to such (and perhaps other) possibilities, it is necessary in a general study to include an additional parameter to properly quantify new physics effects in the gluon fusion channel. For the two-photon amplitude, this parameter can well be different, since new physics can be quite different in the coloured and non-coloured sectors.

With this in view, we parametrize the gluon-gluon-Higgs and Higgs-photon-photon amplitudes as follows:

$$\begin{aligned} \mathcal{L}_{gg}^{eff} &= -x_g f(\alpha_u) \frac{\alpha_s}{12\pi v} H G_{\mu\nu}^a G^{a\mu\nu} \\ \mathcal{L}_{\gamma\gamma}^{eff} &= -x_\gamma g(\alpha_u, \alpha_d, \beta_W, \delta) \frac{\alpha_{em}}{8\pi v} H F_{\mu\nu} F^{\mu\nu} \end{aligned} \quad (7)$$

where x_g and x_γ encapsulate the overall modification due to new intermediate states in the two cases ². The functions $f(\alpha_u)$ and $g(\alpha_u, \alpha_d, \beta_W, \delta)$ encapsulate the modifications of these

²This is just one way of parametrizing the effects of new states. It could be parametrized alternatively adding terms of the form $x_g H G_{\mu\nu}^a G^{a\mu\nu}$ or $x_\gamma H F_{\mu\nu} F^{\mu\nu}$ to the SM Lagrangian. It is straightforward to translate the limits obtained using one convention into those using the other.

couplings due to fermion and W-boson loops. We shall discuss their detailed forms in the next section when we discuss the departures of the Higgs production and decay widths from their SM values in detail. Since there is no restriction till now on x_g and x_γ , we let each of them vary from 0.2 to 3.0. The lower and upper bounds have been set keeping in mind that we do not have too much room for varying them beyond a range, and still being consistent with the data.

Invisible width

Since the earlier analyses of the 2011 data have led to different conclusions about a possible invisible width of the Higgs [7], we keep this possibility alive in our analysis. Such an invisible width can occur if, for example, the Higgs serves as a portal to a ‘dark matter’ sector. The exact expression of the width in terms of the coupling to the dark sector will require one to know the nature of the invisible particle(s), for example, whether they are scalars or spin-1/2 objects. In order to be model-independent, we take as a free parameter the *invisible width* Γ_{inv} , which is independent of the nature of the invisible state, and is also not entangled with other new physics effects.

Since there is very little guideline on the range over which Γ_{inv} should be varied in order to obtain the value corresponding to the minimum of chi-squared, we start from ϵ , the invisible branching ratio, and let it vary between 0 and 1. In each case, the invisible width is expressed as

$$\Gamma_{inv} = \frac{\epsilon}{1 - \epsilon} \sum \Gamma_{vis} \quad (8)$$

where $\sum \Gamma_{vis}$ is the total decay width into all visible channels.

3 Methodology of analysis

3.1 Input data

Table 1 contains the details of all the data points used in our analysis. This includes the combination of 7 TeV (with 5.1 fb^{-1} data) and 8 TeV (with 5.3 fb^{-1} data) results from CMS [1, 9] in all channels, namely, $\gamma\gamma$ (inclusive), $ZZ^* \rightarrow 4\ell$, $WW^* \rightarrow \ell\ell\nu\nu$, $\gamma\gamma jj$, $\tau^+\tau^-$ and $b\bar{b}$. For the ATLAS experiment [2, 9], the $\gamma\gamma$ and ZZ^* results are available as similar 7 + 8 TeV combinations, whereas the 2011 results alone have been used for the remaining channels. The integrated luminosities for ATLAS are 4.9 fb^{-1} and 5.9 fb^{-1} for the 7 and 8 TeV runs respectively. The $\gamma\gamma jj$ results from ATLAS are not yet available. Furthermore, we have used the Tevatron (combined CDF and D0) results for WW^* , $\gamma\gamma$ and $b\bar{b}$, for an integrated luminosity of 10 fb^{-1} [10]. Thus we have fourteen input data points altogether for our global analysis. All the SM production cross-sections and decay widths for the Higgs have been taken from the results reported by the LHC Higgs Cross Section Working Group [13].

In calculating the modifications of various branching ratios of the Higgs, we have used $m_t = 173.5 \text{ GeV}$, $m_b = 4.7 \text{ GeV}$, $m_\tau = 1.777 \text{ GeV}$ and $m_W = 80.4 \text{ GeV}$ [14]. The best fit value for the Higgs mass (m_H) reported by CMS is $125.3 \pm 0.6 \text{ GeV}$ [1], whereas it is 126.5

| Experiment | Channel | $\hat{\mu}$ | M_H (GeV) | Energy (TeV) |
|------------|-----------------------------------------------------|-------------------------|-------------|--------------|
| Tevatron | $H \rightarrow W^+W^-$ | $0.32^{+1.13}_{-0.32}$ | 125 | 1.96 |
| | $H \rightarrow b\bar{b}$ | $1.97^{+0.74}_{-0.68}$ | | |
| | $H \rightarrow \gamma\gamma$ | $3.62^{+2.96}_{-2.54}$ | | |
| ATLAS | $H \rightarrow \gamma\gamma$ | $1.9^{+0.50}_{-0.50}$ | 126.5 | 7 + 8 |
| | $H \rightarrow ZZ^* \rightarrow 4l$ | $1.3^{+0.60}_{-0.60}$ | 126.5 | 7 + 8 |
| | $H \rightarrow WW^* \rightarrow l^+l^-\nu\bar{\nu}$ | $0.52^{+0.57}_{-0.60}$ | 126 | 7 |
| | $H \rightarrow \tau\bar{\tau}$ | $0.16^{+1.72}_{-1.84}$ | 126 | 7 |
| | $H \rightarrow b\bar{b}$ | $0.48^{+2.17}_{-2.12}$ | 126 | 7 |
| CMS | $H \rightarrow \gamma\gamma$ | $1.56^{+0.43}_{-0.43}$ | 125.3 | 7 + 8 |
| | $H \rightarrow ZZ^* \rightarrow 4l$ | $0.7^{+0.40}_{-0.40}$ | | |
| | $H \rightarrow WW^* \rightarrow l^+l^-\nu\bar{\nu}$ | $0.62^{+0.43}_{-0.45}$ | | |
| | $H \rightarrow \tau\bar{\tau}$ | $-0.14^{+0.76}_{-0.73}$ | | |
| | $H \rightarrow b\bar{b}$ | $0.15^{+0.73}_{-0.66}$ | | |
| | $H \rightarrow \gamma\gamma jj$ | $1.58^{+1.06}_{-1.06}$ | | |

Table 1: Input data set used in our analysis, with the values of $\hat{\mu}_i$ in various channels and their 1σ uncertainties as reported by the ATLAS, CMS and Tevatron collaborations.

GeV [2] for ATLAS. The average of these two values, namely, 125.9 GeV has been used by us, in line with, for example, Ref. [15]. For the Tevatron analysis, $m_H = 125$ GeV has been used, following combined CDF and D0 analysis as reported in Ref. [10].

3.2 Methodology

Experimental collaborations have reported various observed signal strengths in the i^{th} channel in terms of $\hat{\mu}_i = \sigma_i^{obs}/\sigma_i^{SM}$, with σ_i as the respective uncertainty. Here, σ_i^{obs} refers to the observed signal cross-section for a particular Higgs mass, while σ_i^{SM} is the signal cross-section for an SM Higgs with the same mass. We calculate the corresponding values of μ_i for various points in the space spanned by the parameters in terms of which we have tried to capture the departure of the Higgs interactions from their SM values, as explained in the previous section. One can express μ_i as

$$\mu_i = R_i^{prod} \times R_i^{decay} / R^{width} \quad (9)$$

where R_i^{prod} , R_i^{decay} and R^{width} are the factors modifying the corresponding SM production cross-sections, decay width in a particular channel, and the total decay width of the Higgs

respectively.

The relevant production mechanisms at the LHC and Tevatron for the various channels are listed below:

- For $\gamma\gamma$ (inclusive), $ZZ^* \rightarrow 4\ell$, $WW^* \rightarrow \ell\ell\nu\nu$ and $\tau^+\tau^-$, one has to include all the production processes, namely, gluon fusion, vector boson fusion, associated WH and ZH production, and Higgsstrahlung from top-antitop pairs.
- Only the associated WH and ZH production channels can lead to $b\bar{b}$ final states that can be separated from backgrounds.
- VBF and GF are the dominant production modes for the $\gamma\gamma jj$ channel reported by CMS; in particular, the contribution of VBF dominates once the appropriate cuts to identify forward tagged jets are imposed. This is reflected in the corresponding efficiencies: 15% for VBF, and 0.5% for GF [18].

In the most general case, the production cross-sections in the gluon fusion (GF), associated production with a Z (ZH), associated production with W^\pm (WH) and associated production with $t\bar{t}$ ($t\bar{t}H$) are modified by the factors $x_g^2\alpha_u^2 (R_{GF})$, $\beta_Z^2 (R_{ZH})$, $\beta_W^2 (R_{WH})$ and $\alpha_u^2 (R_{t\bar{t}H})$ respectively. In the vector boson fusion (VBF) channel, the corresponding factor is given by

$$R_{VBF} \simeq \frac{3\beta_W^2 + \beta_Z^2}{4} \quad (10)$$

The factor R_{VBF} requires some explanation. In order to obtain this, first of all, we have used the fact that the interference of the WW-fusion and the ZZ-fusion diagrams is of the order of 1%, and can therefore be ignored in our calculation. Secondly, the WW-fusion contribution to the total cross-section is roughly 3 times that of the ZZ-fusion contribution. For details on this point we refer the reader to Ref. [16]. We have cross-checked these facts for the LHC energies using the VBF@NNLO code of Bolzoni *et al* [17].

Note that these factors can only be used for inclusive channels of Higgs search, whereby the efficiencies for event selection are the same in various production modes. For channels in which special kinematic selection criteria are used, one has to also include the corresponding efficiency factors, as explained below for the $\gamma\gamma jj$ channel included by CMS.

For the $\gamma\gamma jj$ channel reported by CMS, we have considered VBF and GF as the two most dominant production modes. As reported by CMS, the overall acceptance times selection efficiency of the dijet tag for Higgs boson events is 15% for VBF (ξ_{VBF}) and 0.5% for GF (ξ_{GF}). Therefore, for the VBF channel, the factor modifying the SM production cross-section is given by

$$R_{Hjj} = \frac{\xi_{VBF}R_{VBF}\sigma_{VBF}^{SM} + \xi_{GF}R_{GF}\sigma_{GF}^{SM}}{\xi_{VBF}\sigma_{VBF}^{SM} + \xi_{GF}\sigma_{GF}^{SM}} \quad (11)$$

Next, we consider the Higgs decay widths in the channels under study. The Higgs decay widths in the ZZ^* , WW^* , $\tau\bar{\tau}$, $b\bar{b}$, $c\bar{c}$ and gg channels get multiplied by $\beta_Z^2, \beta_W^2, \alpha_d^2, \alpha_d^2, \alpha_u^2$ and $x_g^2\alpha_u^2$ respectively. In the loop-induced $\gamma\gamma$ channel, the contribution due to the top quark

and W-boson loops (and a small contribution due to the bottom and tau loops) to the Higgs decay width is modified by the factor given by

$$R_{\gamma\gamma} = x_\gamma^2 \frac{|\frac{4}{3}\alpha_u e^{i\delta} A_{1/2}^H(\tau_t) + \frac{1}{3}\alpha_d A_{1/2}^H(\tau_b) + \alpha_d A_{1/2}^H(\tau_\tau) + \beta_W A_1^H(\tau_W)|^2}{|\frac{4}{3}A_{1/2}^H(\tau_t) + \frac{1}{3}A_{1/2}^H(\tau_b) + A_{1/2}^H(\tau_\tau) + A_1^H(\tau_W)|^2} \quad (12)$$

where the relevant loop functions are given by [16]

$$\begin{aligned} A_{1/2}^H(\tau_i) &= 2[\tau_i + (\tau_i - 1)f(\tau_i)]\tau_i^{-2} \\ A_1^H(\tau_i) &= -[2\tau_i^2 + 3\tau_i + 3(2\tau_i - 1)f(\tau_i)]\tau_i^{-2} \end{aligned} \quad (13)$$

Here, $f(\tau_i)$, for $\tau_i \leq 1$ is expressed as,

$$f(\tau_i) = (\sin^{-1} \sqrt{\tau_i})^2 \quad (14)$$

while, for $\tau_i > 1$, it is given by

$$-\frac{1}{4} \left[\log \frac{1 + \sqrt{1 - \tau_i^{-1}}}{1 - \sqrt{1 - \tau_i^{-1}}} - i\pi \right]^2 \quad (15)$$

In the above equations τ_i denotes the ratio $m_H^2/4m_i^2$.

With the values of μ_i thus calculated for various points in the parameter space, we first obtain the best fit values for these parameters (upto 7 at a time) corresponding to the global minimum of the function χ^2 , defined as

$$\chi^2 = \sum_i \frac{(\mu_i - \hat{\mu}_i)^2}{\sigma_i^2} \quad (16)$$

Note that, the experimental collaborations, in some cases, have reported asymmetric error bars on the data. In order to include such error bars in the above definition, we use the following prescription. If $(\mu_i - \hat{\mu}_i) > 0$, we use the positive error bar σ_i^+ , while if $(\mu_i - \hat{\mu}_i) < 0$, we use the negative error bar σ_i^- [19]. Note that, in cases for which we have combined more than one experimental data points to obtain a single input data, we obtained the average signal strength $\bar{\mu}$ and the corresponding uncertainty $\bar{\sigma}$ using the following relations:

$$\begin{aligned} \frac{1}{\bar{\sigma}^2} &= \sum_i \frac{1}{\sigma_i^2} \\ \frac{\bar{\mu}}{\bar{\sigma}^2} &= \sum_i \frac{\hat{\mu}_i}{\sigma_i^2} \end{aligned} \quad (17)$$

This method has been used, for example, in case of CMS data on inclusive $\gamma\gamma$ and $\gamma\gamma jj$ channels, where the results were presented in four different categories in the former case while with both loose and tight dijet tags in the latter case [18].

We have also used the above method in combining different contributions to the theoretically calculated μ values, for example, while combining the contributions of $WH \rightarrow l\nu b\bar{b}$,

| Case | β_W | β_Z | α_u | α_d | x_g | x_γ | ϵ | δ |
|------|-----------|-----------|------------|------------|-------|------------|------------|----------|
| A | 1.2 | 1.6 | -0.6 | -1.2 | 1.8 | 1.3 | 0.6 | 0* |
| B | 1.06 | 1.06 | -1.05 | 0.95 | 0.8 | 1.0 | 0.2 | 0.55 |
| C | 1.07 | 1.07 | -1.3 | -0.96 | 0.65 | 0.95 | 0.2 | 0* |

Table 2: Best-fit values of the various parameters in the three cases considered. In cases A and C, δ has been fixed at 0 (indicated with a '*'). In cases B and C, the relation $\beta_W = \beta_Z$ has been imposed, and their values have been restricted within precision constraints.

$ZH \rightarrow l^+l^-b\bar{b}$ and $ZH \rightarrow \nu\bar{\nu}b\bar{b}$ to associated Higgs production with gauge bosons and the subsequent decay of the Higgs to a bottom pair [13, 20]. Such combinations were necessitated by the fact that the experimental collaborations have reported a single signal strength value in the $b\bar{b}$ channel.

After obtaining the best-fit values for the parameters by minimizing the χ^2 function, we consider two-dimensional contours for various pairs of them about the global minimum, fixing the remaining ones at their best-fit values. The contours are drawn for 68.3% and 95.4% confidence intervals. One important point in which our study differs from most earlier ones is that, in the cases where these two-dimensional contours are drawn, *the remaining parameters are fixed not at their SM values but at values corresponding to the global minimum of the χ^2 fit*. The various values of $\Delta\chi^2$ for the 68.3% and 95.4% confidence intervals are tabulated, for example, in Refs. [21, 22].

4 Results

We obtain the global fits in three different cases. In the first case (case A), the phase δ is set to zero, and the seven remaining parameters are varied across the pre-decided ranges, as described in section 2. In the second case (case B), we try to see the effects of the phase, and set $\beta_W = \beta_Z$ in the process. The same exercise is done in the third case, but with the phase set to zero again. The simplification in the last two cases is done because $\beta_W \neq \beta_Z$ amounts to the breaking of custodial SU(2) at the tree-level, and is subject to rather stringent constraints from precision electroweak observables. Though we go beyond these constraints in the first case, assuming the simultaneous existence of more than one gauge-invariant effective interactions at the same time, we desist from such speculative exercise in the cases B and C, and keep $\beta_W = \beta_Z$ within the most stringent precision electroweak limits. It should be noted that the phase δ does not affect the loop-induced contribution to the T-parameter, since it cancels in the relevant self-energy diagrams. Table 2 contains the best fit values of various parameters in the three cases.

The obtained best-fit values for the parameters have been tabulated in Table 2. The minimum values of χ^2 , χ^2_{min} are 6.19, 7.03 and 7.03 for cases A, B and C respectively. Note that, the number of degrees of freedom (for cases A and B) in our global fits is 7, since we

have 14 input data points, and 7 parameters. However, for case C the number of degrees of freedom is 8, since $\beta_W = \beta_Z$ and $\delta = 0$. We present the two-dimensional 68.3% and 95.4% confidence interval contours for various pairs of parameters about the global minimum, for cases A and B, in Figures 1 and 2 respectively. As mentioned before, while drawing these contours, we have fixed the remaining parameters at their best-fit values. In this connection, we note that the consistency of our methodology has been checked by also performing a two parameter fit of the data (with the parameters pertaining to the overall modifications of the fermion and gauge couplings), and our results in that case agree with those presented in recent literature [8].

Let us first consider the case with $\delta = 0$ and $\beta_W \neq \beta_Z$. First of all, there is a global tendency in the experimental results reported so far towards best fit values of the WW rates that are consistent with a shortfall compared to the SM prediction. For ZZ, on the other hand, there is an excess for ATLAS and a shortfall, but less than that for WW, for CMS. Though these are all consistent at the 1σ level, the least-square minimisation inevitably yields a best fit for β_Z higher than that of β_W . Since this causes one to go beyond the most stringent of precision constraints, one has to admit that such a best fit central value favours the simultaneous presence of more than one gauge-invariant anomalous WW/ZZ interactions for the Higgs. It should, of course, be kept in mind that one has to wait for the accumulation of more data before a final verdict can be spelt on this. In cases B and C, where we set $0.92 \leq \beta \leq 1.18$, with $\beta \equiv \beta_W = \beta_Z$, we find the best-fit values of β to be close to 1.

As far as the best fit values for the parameters multiplying the fermion couplings are concerned, we find that α_u receives a sign relative to β_W , with a value -0.6 , -1.05 and -1.3 for cases A, B and C respectively. This relative sign between the top-quark Yukawa coupling and the W-boson coupling to the Higgs can be traced to the fact that the observed excess in the $\gamma\gamma$ mode by both the ATLAS and CMS experiments can be explained by a constructive interference between the loop amplitudes due to the top and the W-loop. In contrast to α_u , the magnitude of the best-fit value of α_d in all cases turns out to be close to unity. Its sign does not affect the Higgs production cross-sections and decay branching ratios much, except for a small effect in the $\gamma\gamma$ decay mode. However, to be completely general, we varied it in the range -2.0 to 2.0 . One should note that, as can be seen in Figure 1, the 68% and 95% contours allow for both positive and negative values of α_d , and these contours bring out the global picture more clearly than just the best-fit values. It should be noted that α_d has a positive best fit value only when the phase δ is turned on. This elicits an interesting feature of the global fit, when the phase in fermion couplings is included. We also note that, from contours involving α_u and α_d in Figure 1 and α_u in Figure 2, it is clear that values close to zero of these two parameters are clearly disfavoured. This, therefore, should severely constrain fermiophobic models for the Higgs [23].

We also find the best-fit values for x_g and x_γ to differ, and at the same time lie away from their SM value of 1.0. This suggests that not only is the presence of new coloured or electrically charged states coupling to the Higgs plausible, but that the number of states contributing to the gluon fusion process can be different from those contributing to the $\gamma\gamma$ decay mode.

In case A, we find a rather large allowed value for the invisible branching ratio of the Higgs boson. This may be due to the fact that the production rate in the gluon fusion channel, as well as the Z boson contribution to the associated production and VBF processes (as the

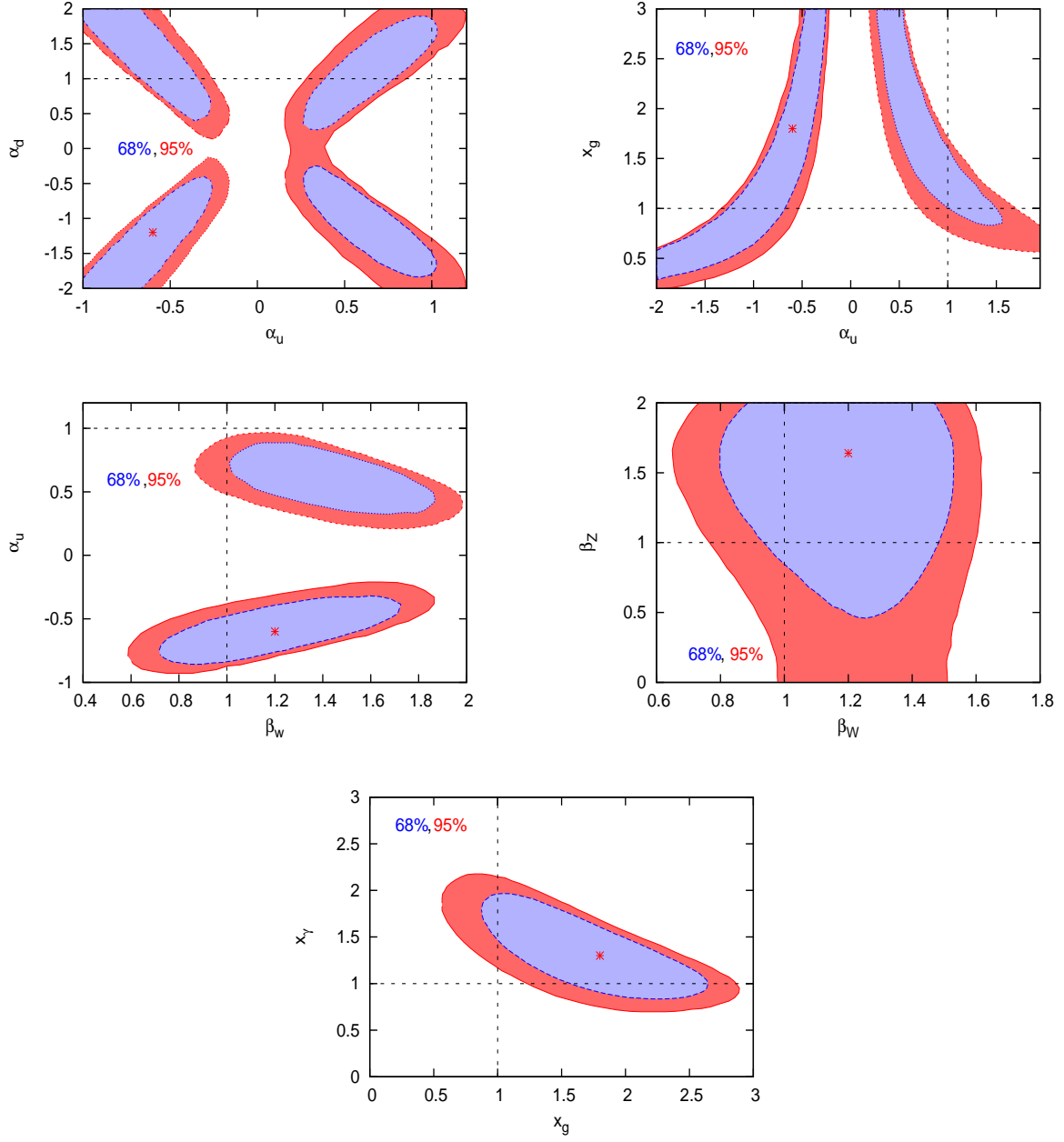


Figure 1: Two-dimensional contour plots for 68% and 95% confidence intervals, for case A, with rest of the parameters fixed at their best-fit values. The best-fit point is also marked separately by a '*'. In this case δ has been fixed at 0, whereas $0 \leq \beta_w, \beta_z \leq 2.0$, and $\beta_w \neq \beta_z$.

best-fit of β_z is 1.6) are enhanced. This creates room for the simultaneous enhancement of

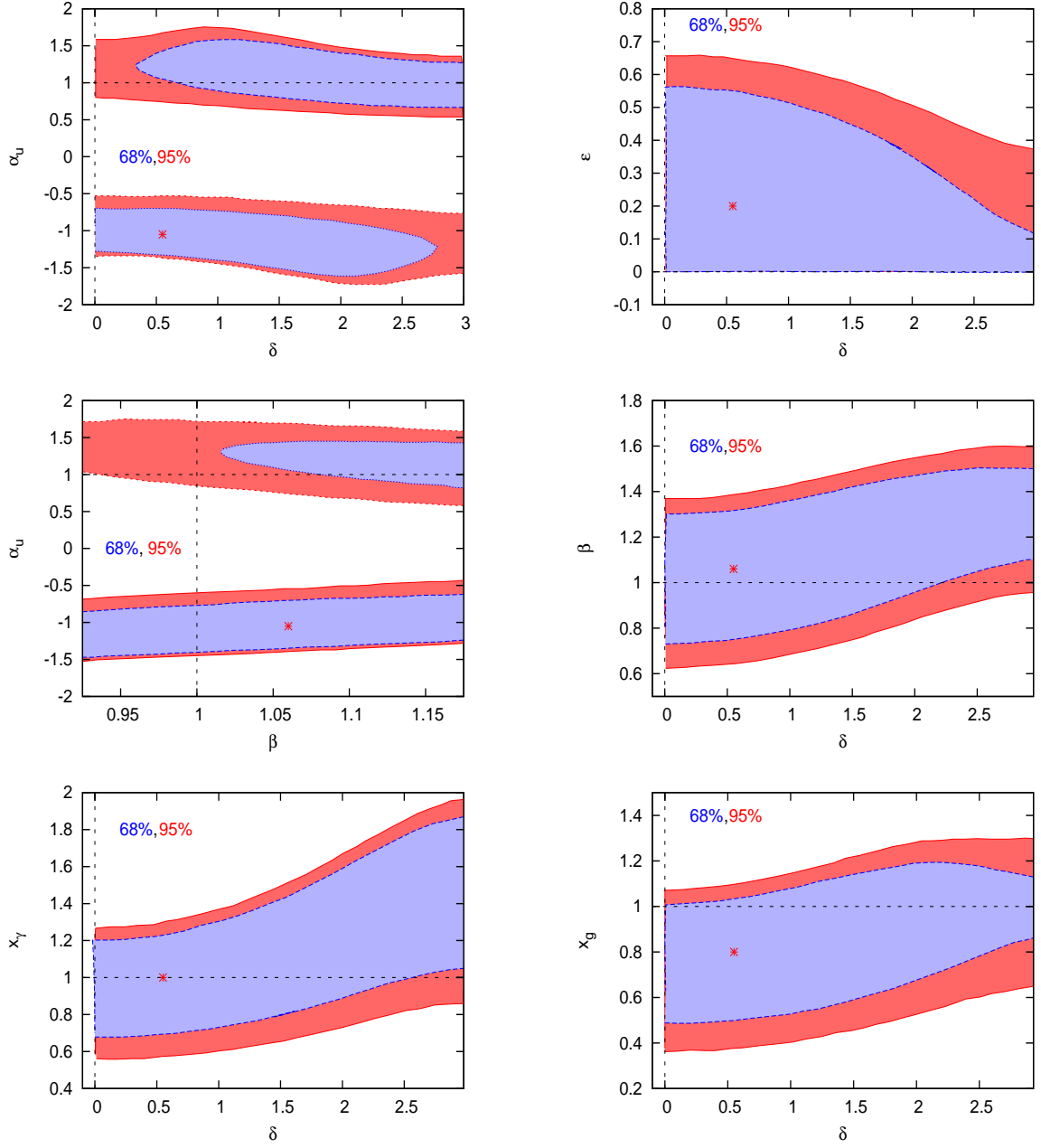


Figure 2: Two-dimensional contour plots for 68% and 95% confidence intervals, for case B, with rest of the parameters fixed at their best-fit values. The best-fit point is also marked separately by a '*'. In this case δ has been varied in the range $\{0, \pi\}$, whereas $0.92 \leq \beta \leq 1.18$, with $\beta \equiv \beta_W = \beta_Z$.

certain visible modes ($\gamma\gamma, ZZ^*$) as well as the existence of substantial invisible branching

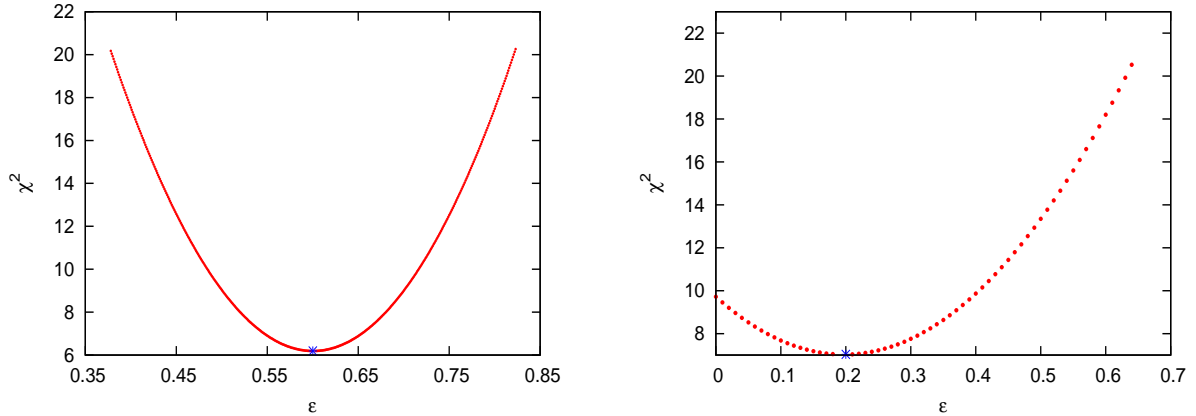


Figure 3: Variation of the χ^2 function with the invisible branching fraction of H (ϵ) in cases A (left panel) and B (right panel). In case A, $\delta = 0$ and $\beta_W \neq \beta_Z$, whereas in case B, δ has been varied in the range $\{0, \pi\}$ and $0.92 \leq \beta \leq 1.18$, with $\beta \equiv \beta_W = \beta_Z$.

fraction. Note that we observe a reduction in ϵ once β_W and β_Z are set to be equal, and in the range allowed by electroweak precision data (cases B and C), the best-fit value in both these cases being 0.2. Thus our conclusion is that, while invisible decays of the Higgs are more constrained once a correlation between the HWW and HZZ couplings is enforced, the overall freedom in a seven-parameter space nonetheless keeps enough scope for such decays. We demonstrate the variation of the χ^2 function with ϵ , in cases A and B, with rest of the parameters fixed at their best-fit values, in Figure 3.

The interesting feature to be noted is that the phase δ is allowed to assume values as large as 0.55 in the best fit. Once this non-trivial phase is there, the 95% confidence level contours of all other anomalous interactions tend to include the SM values. It should however be also noted from Figure 4 that although the best fit value for δ is 0.55, the χ^2 function is very slowly varying in the entire range between 0 and 0.6. The curve as a whole indicates that the best fit value is relatively unspecified between 0 and 1, and we have to wait for more data to have a clearer picture about the occurrence of this phase. Also, a comparison between the $\alpha_u - \beta_W$ plot in Figure 1 and the $\alpha_u - \beta$ plot in Figure 2 shows that the contours not only shift but have also bigger coverage in the $\delta \neq 0$ case.

5 Summary and conclusions

The attempt in this study is to see how much scope of new physics is contained within the data on Higgs search, taking into account not only the results available from 7 and 8 TeV runs of the LHC but also the full data set of the Tevatron. We have taken a completely model-independent stand, without any bias of correlation between the anomalous Higgs couplings of $T_3 = +1/2$ and $-1/2$ fermions, as well as the W- and Z-couplings. We have

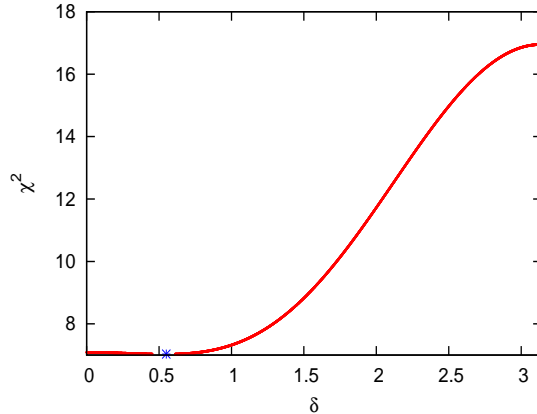


Figure 4: Variation of the χ^2 function with the phase in the up-type quark Yukawa coupling, δ , in case B. In this case δ has been varied in the range $\{0, \pi\}$, whereas $0.92 \leq \beta \leq 1.18$, with $\beta \equiv \beta_W = \beta_Z$.

in addition accounted for additional states contributing to the effective interaction of the Higgs with photon and gluon pairs. Since such contributions can come through different sets of states for the gg and $\gamma\gamma$ pairs, we assign a separate uncorrelated parameter for each of these processes. Furthermore, we have taken into account an arbitrary phase in the top-pair coupling with respect to that from a W-pair, which can in principle non-trivially affect the loop-induced decay $H \rightarrow \gamma\gamma$. Last but not the least, a non-vanishing width for the Higgs decaying into invisible final states is kept as a free parameter in our global fit.

Our study takes into account not only the contributions to all final states from the dominant gluon fusion channel but also the VBF and all associated production subprocesses, with appropriate weightage to the efficiencies for different channels. Also, asymmetric uncertainties in the data, as reported by the experiments in some cases, have been used in our analysis. The present study is nonetheless based on certain simplifying assumptions. These include, for example, the same cut efficiencies taken in inclusive final states where more than one production channels are involved, which can be improved as and when the efficiencies are published by the experimental collaborations.

The global fits for the minimum of χ^2 over seven-parameter scans, for three sets of combinations, yield the best fit values of each. Subsequently, 68% and 95% confidence level contours for various parameters have been presented, where all other parameters have been kept at their global best fit values (in contrast to most studies where they are fixed at the corresponding SM values).

The most important conclusion we draw is that it is too early to say that signals reveal *the standard model Higgs*, since the 2σ contours allow departure from the SM values. A few general trends that show up are

- A fermiophobic Higgs is by and large disfavoured.

- There is in general the hint in the best-fit values of a relative sign between the couplings to the up-type fermion and the gauge boson pairs.
- A non-trivial phase in the top-quark coupling can have a rather important role. Interestingly, the SM values of the remaining parameters tend to get included within the 2σ contours once this phase is turned on.
- It still seems possible to accommodate an invisible decay width of the Higgs. In particular, it can be as large as 60% if one allows a breakdown of the custodial SU(2) symmetry. Though this is *prima facie* restricted by electroweak precision data, it remains to be checked whether the values of $\beta_W \neq \beta_Z$ can be made consistent with precision data, by introducing more than one gauge invariant higher-dimensional operators at the same time. However, invisible branching ratios upto 20% or more are possible even without such manoeuvres.

Data from the LHC are currently in a state of flux, and therefore the numerical results on which our analysis is based can change with growing statistics. However, while the trends pointed out by us might change as more accurate data become available, the rather general approach used by us should continue to serve as a template for future analyses.

Acknowledgement

We thank Satyaki Bhattacharya, Frederick James and Lorenzo Moneta for many valuable discussions and useful correspondence. We would also like to thank Dhiraj Kumar Hazra for an important computational help. S.B. and B.M. thank the Indian Association for the Cultivation of Science, Kolkata, for hospitality while this study was in progress. This work was partially supported by funding available from the Department of Atomic Energy, Government of India for the Regional Centre for Accelerator-based Particle Physics, Harish-Chandra Research Institute. Computational work for this study was partially carried out at the cluster computing facility in the Harish-Chandra Research Institute (<http://cluster.hri.res.in>).

References

- [1] J. Incandela, talk on behalf of the CMS Collaboration at CERN, 4th July, 2012, <https://cms-docdb.cern.ch/cgi-bin/PublicDocDB//ShowDocument?docid=6125>.
- [2] F. Gianotti, talk on behalf of the ATLAS Collaboration at CERN, 4th July, 2012, <https://cms-docdb.cern.ch/cgi-bin/PublicDocDB//ShowDocument?docid=6126>.
- [3] S. L. Glashow, Nucl. Phys. **22**, 579 (1961); S. Weinberg, Phys. Rev. Lett. **19**, 1264 (1967); A. Salam, Proceedings of 8th Nobel Symposium, Ed. N. Svartholm (1968).
- [4] F. Englert and R. Brout, Phys. Rev. Lett. **13** (1964) 321; P. W. Higgs, Phys. Rev. Lett. **13** (1964) 508; P. W. Higgs, Phys. Lett. **12** (1964) 132; G. S. Guralnik, C. R. Hagen

- and T. W. B. Kibble, Phys. Rev. Lett. **13** (1964) 585; P. W. Higgs, Phys. Rev. **145** (1966) 1156-1163; T. W. B. Kibble, Phys. Rev. **155** (1967) 1554-1561.
- [5] A. Azatov, R. Contino and J. Galloway, JHEP **1204**, 127 (2012).
- [6] M. Farina, C. Grojean, E. Salvioni, arXiv:1205.0011 [hep-ph];
- [7] J.R. Espinosa, C. Grojean, M. Muhlleitner and M. Trott, arXiv:1202.3697 [hep-ph]; P. P. Giardino, K. Kannike, M. Raidal and A. Strumia, arXiv:1203.4254 [hep-ph]; T. Li, X. Wan, Y. Wang and S. Zhu, arXiv:1203.5083 [hep-ph]; M. Rauch, arXiv:1203.6826 [hep-ph]; J.R. Espinosa, M. Muhlleitner, C. Grojean and M. Trott, arXiv:1205.6790 [hep-ph]; J. Ellis and T. You, JHEP **1206** (2012) 140; D. Carmi, A. Falkowski, E. Kuflik and T. Volanski, arXiv:1202.3144 [hep-ph]; M. Duhrssen, S. Heinemeyer, H. Logan, D. Rainwater, G. Weiglein and D. Zeppenfeld, Phys. Rev. D **70** (2004) 113009; R. Lafaye, T. Plehn, M. Rauch, D. Zerwas and M. Duhrssen, JHEP **0908** (2009) 009; M. Klute, R. Lafaye, T. Plehn, M. Rauch and D. Zerwas, arXiv:1205.2699 [hep-ph]; A. Azatov, R. Contino, D. Del Re, J. Galloway, M. Grassi and S. Rahatlou, arXiv:1204.4817 [hep-ph].
- [8] I. Low, J. Lykken and G. Shaughnessy, arXiv:1207.1093 [hep-ph]; T. Corbett, O. J. P. Eboli, J. Gonzalez-Fraile and M.C. Gonzalez-Garcia, arXiv:1207.1344 [hep-ph]; P.P. Giardino, K. Kannike, M. Raidal and A. Strumia, arXiv:1207.1347 [hep-ph]; J. Ellis and T. You, arXiv:1207.1693 [hep-ph]; J. R. Espinosa, C. Grojean, M. Muhlleitner and M. Trott, arXiv:1207.1717 [hep-ph]; M. Montull and F. Riva, arXiv:1207.1716 [hep-ph]; D. Carmi, A. Falkowski, E. Kuflik, T. Volansky and J. Zupan, arXiv:1207.1718 [hep-ph]; J. Baglio, A. Djouadi and R. M. Godbole, arXiv:1207.1451 [hep-ph].
- [9] G. Aad *et al.* [ATLAS Collaboration], Phys. Lett. B **710** (2012) 49; S. Chatrchyan *et al.* [CMS Collaboration], Phys. Lett. B **710** (2012) 26; CMS Collaboration, Phys. Rev. Lett. **108** (2012) 111804; ATLAS Collaboration, Phys. Lett. B **710** (2012) 383-402; ATLAS Collaboration, Phys. Rev. Lett. **108** (2012) 111803; CMS Collaboration, Phys. Lett. B **710** (2012) 91-113; CMS Collaboration, arXiv:1202.4083 [hep-ex];
- [10] Tevatron New Physics Higgs Working Group and CDF and D0 Collaborations, arXiv:1207.0449 [hep-ex].
- [11] K. Hagiwara, S. Ishihara, R. Szalapski and D. Zeppenfeld, Phys. Lett. B **283**, 353 (1992); K. Hagiwara, S. Ishihara, R. Szalapski and D. Zeppenfeld, Phys. Rev. D **48**, 2182 (1993).
- [12] M. C. Gonzalez-Garcia, Int. J. Mod. Phys. A **14**, 3121 (1999).
- [13] S. Dittmaier *et al.* [LHC Higgs Cross Section Working Group Collaboration], arXiv:1101.0593 [hep-ph]; S. Dittmaier *et al.*, arXiv:1201.3084 [hep-ph]; <https://twiki.cern.ch/twiki/bin/view/LHCPhysics/CrossSections>
- [14] J. Beringer *et al.* (Particle Data Group), Phys. Rev. D **86**, 010001 (2012).

- [15] A. Arbey, M. Battaglia, A. Djouadi and F. Mahmoudi, arXiv:1207.1348 [hep-ph].
- [16] A. Djouadi, Phys. Rept. **457**, 1 (2008).
- [17] P. Bolzoni, F. Maltoni, S. -O. Moch and M. Zaro, Phys. Rev. Lett. **105**, 011801 (2010); Phys. Rev. D **85**, 035002 (2012); <http://vbf-nnlo.phys.ucl.ac.be/vbf.html>
- [18] S. Chatrchyan *et al.* [CMS Collaboration], Phys. Lett. B **710**, 403 (2012).
- [19] F. James, private communication.
- [20] J. Baglio and A. Djouadi, JHEP **1010**, 064 (2010).
- [21] <http://seal.web.cern.ch/seal/snapshot/work-packages/mathlibs/minuit/>
- [22] W. H. Press *et al.*, Numerical Recipes in Fortran, Cambridge University Press (2005).
- [23] E. Gabrielli, B. Mele and M. Raidal, arXiv:1202.1796 [hep-ph], and references therein.